Journal of Colloid and Interface Science 518 (2018) 216–224

Contents lists available at ScienceDirect

Journal of Colloid and Interface Science

journal homepage: www.elsevier.com/locate/jcis

Regular Article

Effect of small molecules on the phase behavior and coacervation of aqueous solutions of poly(diallyldimethylammonium chloride) and poly (sodium 4-styrene sulfonate)

Shuyue Huang [a,1], Mengmeng Zhao [a,1], Mahesh B. Dawadi [b], Yuhang Cai [c], Yakov Lapitsky [c], David A. Modarelli [b], Nicole S. Zacharia [a,*]

[a] Department of Polymer Engineering, University of Akron, Akron, OH 44325, United States
[b] Department of Chemistry, University of Akron, Akron, OH 44325, United States
[c] Department of Chemical Engineering, University of Toledo, Toledo, OH, 43606, United States

GRAPHICAL ABSTRACT

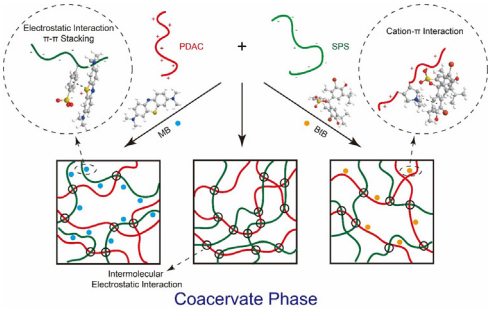

ARTICLE INFO

Article history:
Received 2 December 2017
Revised 7 February 2018
Accepted 8 February 2018
Available online 9 February 2018

Keywords:
Polyelectrolyte coacervation
Electrostatic
Hydrophobic interaction
Separations
Encapsulation

ABSTRACT

Hypothesis: Complex coacervates are capable of easily partitioning solutes within them based on relative affinities of solute-water and solute-polyelectrolyte pairs, as the coacervate phase has low surface tension with water, facilitating the transport of small molecules into the coacervate phase. The uptake of small molecules is expected to influence the physicochemical properties of the complex coacervate, including the hydrophobicity within coacervate droplets, phase boundaries of coacervation and precipitation, solute uptake capacity, as well as the coacervate rheological properties.

Experiments: Phase behavior of aqueous solutions of poly(diallyldimethylammonium chloride) (PDAC) and poly(sodium 4-styrene sulfonate) (SPS) was investigated in the presence of various concentrations of two different dyes, positively charged methylene blue (MB) or non-charged bromothymol blue (BtB), using turbidity measurements. These materials were characterized with UV–vis spectroscopy, zeta potential measurements, isothermal titration calorimetry (ITC), fluorescence spectroscopy, and dynamic rheological measurements.

Findings: The presence of MB or BtB accelerates the coacervation process due to the increased hydrophobicity within coacervates by the addition of MB or BtB. The encapsulated MB or BtB tends to reduce the ionic crosslink density in the PDAC-SPS coacervates, resulting in a much weaker interconnecting network of the PDAC-SPS coacervates.

* Corresponding author.
E-mail address: nzacharia@uakron.edu (N.S. Zacharia).
[1] These authors contributed equally to this work.

https://doi.org/10.1016/j.jcis.2018.02.029
0021-9797/

1. Introduction

It has been long known that the electrostatic interaction of oppositely charged polyelectrolytes can lead to the formation of soluble complexes, or to phase separation including liquid-liquid (coacervation) and liquid-solid (precipitation) separation, depending on factors such as charge density, ionic strength and polymer molecular weight [1–4]. When complex coacervation occurs, a dense polymer-rich phase (coacervate phase) and a very dilute polymer-deficient phase (aqueous phase), which exist in equilibrium, are formed [4–6]. The coacervation process is generally considered to be entropically driven by the release of small counter ions, producing dispersed polyelectrolyte-rich liquid coacervate droplets [4,5,7]. Complex coacervation has been applied in various fields, including pharmaceutical delivery and food industries as microencapsulates for drugs and flavors [8,9]. For example, chitosan-based coacervates have been investigated for the delivery of proteins and vaccines, which provides insight for the development of coacervates for delivery of protein biologics and vaccines [10]. Kohane et al. developed gelatin-gum Arabic complex coacervates for the encapsulation and thermally sensitive controlled release of flavor compounds, to improve the appeal of frozen baked foods upon heating [11].

As the coacervate phase has low surface tension with water, it is capable of easily partitioning solutes within it based on relative affinities between the solute and the polyelectrolytes and water. For example, our previous study shows that complex coacervates formed with oppositely charged polyelectrolytes have the ability to efficiently sequester a cationic dye, methylene blue (MB), through both electrostatic and π-π interactions [12]. Another study on hydrogen-bonding complex coacervates reveals that with the specific hydrogen bonding interaction between the solutes and polymer, the uptake efficiency can be significantly increased. Additionally, by adjusting the hydrophobicity within coacervate droplets, the partition coefficient of solutes can be tuned [13]. These preliminary studies may give insight into better designing polymeric coacervate-based materials for drug delivery or personal care products.

It has been widely reported that the phase behavior of polyelectrolyte aqueous solutions is highly dependent on many factors, *i.e.*, molecular weight, polymer concentration, stoichiometry of the two interacting polyelectrolytes, ionic strength, charge density, as well as the temperature of the solution [1,14,15]. For instance, it was found that upon shortening the chain length of polyelectrolytes, or when there is a significant deviation of the stoichiometric polycation/polyanion ratio, the stability of the complex coacervate phase was decreased [1]. It has been reported that increases in salt concentration can lead to transitions from precipitates to coacervates and finally to polyelectrolyte solutions [1,16]. The precipitate-coacervate transition is regarded as the result of successive replacement of ion pairs between oppositely charged polyelectrolytes. Compared to the precipitate-coacervate transition, the coacervate-solution transition occurs at relatively high salt concentrations, where intermolecular electrostatic interactions have been significantly screened. However, there are few studies on how the sequestered solutes within coacervates would in turn impact the phase behavior and coacervation of aqueous polyelectrolyte systems.

This study provides a more complete understanding of phase behavior and complex coacervation of synthetic, strong polyelectrolytes in the presence of small molecules, using poly(diallyldimethylammonium chloride) (PDAC) as the polycation and poly(sodium 4-styrene sulfonate) (SPS) as the polyanion. The small molecules partitioned into the coacervate in this work are an aromatic cationic water-soluble dye (methylene blue or MB) as well as an aromatic non-ionic dye (bromothymol blue or BtB) into the PDAC-SPS coacervates was studied. These various molecules can be seen in Scheme 1. The influence of the small molecules on the phase boundaries was examined and explained with a number of techniques, including spectrofluorimetry isothermal titration calorimetry (ITC) and rheology to examine the interaction between the dyes and polyelectrolytes, as well as the influence of these dyes on the physical properties of the coacervate. Although works studying how to encapsulate small molecules into coacervates are represented in the literature, there are few if any reports showing how the presence of these small molecules impact phase boundaries or other transitions such as precipitation and rheological properties of the coacervates themselves.

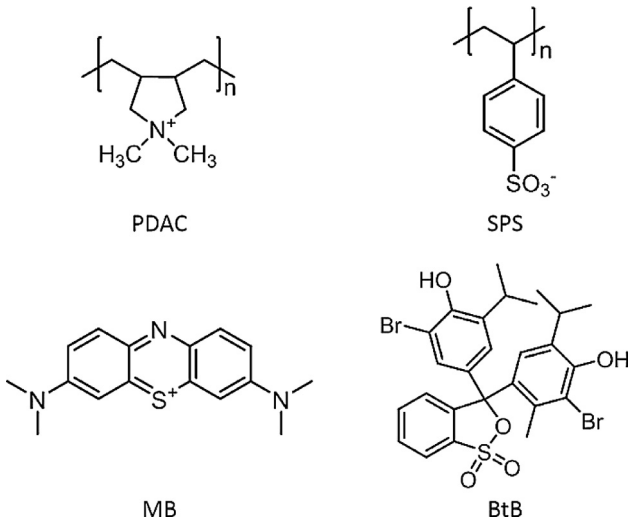

Scheme 1. Chemical structures of PDAC, SPS, MB and BtB.

2. Experimental section

2.1. Materials

Poly(diallyldimethylammonium chloride) (PDAC, $M_n = 16000$, $PDI = 1.4$), poly(sodium 4-styrene sulfonate) (SPS, $M_n = 13000$, PDI = 1.6), and MB, BtB and ANS dyes were purchased from Sigma-Aldrich. The molecular weight and polydispersity of PDAC and SPS were measured by aqueous gel permeation chromatography (GPC) using polyethylene oxide standards. Both the polycation PDAC and the polyanion SPS are strong polyelectrolytes and are insensitive to pH. All water was dispensed from a Milli-Q water system at a resistivity of 18.2 MΩ cm. All these materials were used as received without further purification.

2.2. Turbidity measurement

Turbidity was used to qualitatively measure the extent of coacervate formation as a function of PDAC/SPS stoichiometry (PDAC/SPS) at different total polyelectrolyte concentration, with the addition of various amounts of MB or BtB. The detailed information on the concentration of PDAC and SPS stock solutions with various concentrations of added MB or BtB, namely PDAC-MB and SPS-MB, or PDAC-BtB and SPS-BtB stock solutions, were listed in Tables S1 and S2. Turbidity measurements for the titration with the addition of MB were performed using a 2 cm path length fiber-optic colorimeter (Brinkmann PC 950) at a wavelength of 420 nm. Turbidity measurements for the titration with the addition of BtB were performed on an Agilent 8453 UV–vis Spectrophotometer at a wavelength of 600 nm, to avoid the absorbance of BtB at 420 nm.

Turbidity was reported as 100 – *T*%, where *T* corresponds to the transmittance. Titration of PDAC-dye stock solutions (1, 5, 10, 20, or 40 mM) into SPS-dye stock solutions (1, 5, 10, 20, or 40 mM) with matching polyelectrolyte and dye concentrations was done with stirring. The transmittance (*T*) was recorded at 60 s after each PDAC addition. All of the above polyelectrolyte concentrations are repeat unit concentrations.

2.3. Zeta potential measurement

Zeta potential measurements were used as a way to approximate charge of the coacervate particles in solution. Stock solutions of PDAC (10 mM) and SPS (10 mM) with various concentrations of added MB or BtB (see Table S3) were prepared separately. MB or BtB encapsulated PDAC-SPS coacervates were formed simply by mixing the dye added PDAC and SPS stock solutions with matching dye concentrations at a mixing ratio of PDAC:SPS = 0.5, keeping the total concentration of PDAC and SPS at 10 mM. Stock solutions of PDAC (10 mM) and SPS (10 mM) without dye addition were prepared separately as well. Dye-free PDAC-SPS coacervate samples were prepared by mixing the PDAC and SPS stock solutions at various mixing ratios (PDAC:SPS = 0.067, 0.1, 0.2 and 0.5). The apparent zeta potentials of the as-prepared PDAC-SPS coacervates with various added dye concentrations or various PDAC:SPS molar ratios without dye addition were then estimated using a Brookhaven Instruments Zeta PALS electrophoretic light scattering instrument (where the Smoluchowski model was used to obtain apparent zeta potential values from the measured electrophoretic mobilities).

2.4. Determining partition coefficient of dyes into coacervates

Partition coefficients show the efficiency of a particular coacervate system to encapsulate a dye. Stock solutions of PDAC (10 mM) and SPS (10 mM) were made with the addition of various concentrations of MB or BtB, respectively (see Table S4). PDAC-SPS coacervates with sequestered dyes were prepared by mixing the PDAC and SPS stock solutions with a mixing ratio of PDAC:SPS = 0.5, to study the dye partition coefficients as functions of dye concentration. Further, to examine how these partition coefficients depend on the PDAC:SPS mixing ratio, stock solutions of PDAC (10 mM) and SPS (10 mM) containing 0.01 mM MB were prepared. These solutions were mixed in various ratios to prepare additional batches of PDAC-SPS coacervates with sequestered MB and variable PDAC:SPS mixing ratios (PDAC:SPS = 0.067, 0.1, 0.2 and 0.5). After 24 h stirring, samples were centrifuged for 3 h at 8000 rpm (Allegra X-30R Centrifuge, Beckman Coulter). After centrifugation, the supernatant was removed using a micropipette, and the coacervate phase was left in the bottom of centrifuge tubes. UV–vis measurements (Agilent 8453 spectrophotometer) were used to determine the dye concentration in the supernatant and to then infer it in the coacervate. The partition coefficient (*K*) was calculated as Eq. (1).

$$K = \frac{[Solute\ in\ Coacervate]}{[Solute\ in\ Supernatant]} \quad (1)$$

2.5. Fluorescence spectroscopy

Fluorescence spectrometry was used to measure polarity of the microenvironment within the coacervate. Steady state emission spectra of ANS within PDAC-SPS coacervate microdroplets with or without accumulated MB in coacervate were measured using a Horiba FluoroMax 4 spectrofluorometer with an excitation wavelength of 350 nm. Fluorescence emission was measured from 365 to 650 nm in quartz cuvettes for microdroplet dispersions prepared with 10 mM PDAC and 10 mM SPS with a mixing ratio of PDAC:SPS = 0.5, 0.5 mM of added ANS and different (0, 0.1, 0.5 and 1 mM) concentrations of MB. All fluorescence was attributed to ANS within the microdroplets as ANS fluorescence was quenched in water.

2.6. Rheological measurements

The coacervate samples were prepared by mixing PDAC (5 mM) and SPS (5 mM) at a PDAC:SPS stoichiometry of 0.75 and various MB or BtB concentrations (see Table S5), and collected by centrifuging the mixtures at 8000 rpm for 3 h (Allegra X-30R Centrifuge, Beckman Coulter). The dynamic rheological properties of the collected coacervates were characterized using a TA Instruments ARES-G2 rheometer in parallel plate geometry using an 8.00 mm diameter aluminium upper plate and 43.9 mm diameter aluminium lower plate along with a solvent trap. For dynamic rheological experiments, a constant strain amplitude of 0.4%, which was within the linear viscoelastic response region for all the collected coacervate samples, was used. The frequency was swept from 0.1 to 100 rad/s for these dynamic measurements.

2.7. Isothermal titration calorimetry (ITC)

ITC experiments were performed using a VP-ITC microcalorimeter (GE Healthcare, USA). Each titration experiment involved 27 injections (10 μL) of 2.5 mM polyelectrolyte (either PDAC or SPS) solution at 5 min intervals into the sample cell containing 0.25 mM dye (MB or BtB) solution. Both the polyelectrolyte and dye solutions had the same pH of 3.00 ± 0.02. The reference cell was filled with DI water, while the experimental temperature and stirring rate were fixed at 25 °C and 310 rpm, respectively. The heat of dilution, which was obtained through a control experiment where the PDAC or SPS were titrated into dye-free water at a matching pH, was later subtracted from the titration data to generate the final thermogram that reflected the enthalpic signature of the polyelectrolyte-dye binding.

2.8. Optical microscopy

An optical microscope (Olympus DP80) was used to obtain images of coacervate droplets. The coacervate mixture was centrifuged and then placed on a glass slide to image the droplets. Coacervate and precipitate samples were prepared by adding 10 mM PDAC solution into 10 mM SPS solution with a ratio of 1:4 and 1:1, respectively. Samples used for imaging were centrifuged for 15 min at 8000 rpm using a centrifuge (Allegra X-30R Centrifuge, Beckman Coulter) to achieve rapid sedimentation. After centrifugation, the supernatant was carefully removed by using a micro-pipette while the dense coacervate phase was left at the bottom of centrifuge tube, and transferred on to the glass slide to obtain optical microscope images. Similarly, optical microscope images of precipitate were obtained as well.

2.9. ^1H NMR

^{1}H NMR spectroscopy (Mercury 300 spectrometer) was used to measure the PDAC:SPS ratios in the polyelectrolyte complex coacervates as follows: PDAC-SPS coacervate samples were prepared by mixing the PDAC (10 mM) and SPS (10 mM) stock solutions with various mixing ratios (PDAC:SPS = 0.067, 0.1, 0.2 and 0.5), and collected by centrifuging the mixtures at 8000 rpm for 3 h (Allegra X-30R Centrifuge, Beckman Coulter). The collected coacervate samples were dried at 60 °C to remove water completely. The dried coacervate samples were then dissolved in D_2O with the addition of 2.5 M KBr.

3. Results and discussion

3.1. Solute partitioning into PDAC-SPS coacervates

The partitioning of the two dyes MB and BtB into PDAC-SPS coacervates was studied using UV–vis spectroscopy. Fig. 1 shows the partition coefficients of MB and BtB into PDAC-SPS coacervates as a function of solute concentration, at a fixed mixing ratio of PDAC:SPS = 0.5. The partitioning of MB into the PDAC-SPS complex coacervate is significantly higher than that for BtB. This efficient uptake of MB likely reflects the strong π-π interactions between MB and SPS as previously reported [12]. The UV–vis spectra of pure MB, MB with SPS, pure BtB and BtB with SPS aqueous solution at pH 3.0 are shown in Fig. S1. The red shift in the UV–vis maximum absorbance wavelength (λ_{max}) of MB in the aqueous solution with SPS indicates π-π interaction between MB and SPS. However, there is no shift in λ_{max} of BtB in the aqueous solution with SPS, which suggests that there is no π-π interaction between BtB and SPS. In addition, as the concentration of MB increases from 0.01 to 0.5 mM, the partition coefficient of MB into the PDAC-SPS complex coacervate increases from approximately 120 to 210; even though the apparent zeta potential (which reflects the negative coacervate charge) is reduced from approximately −36 to −5 mV as the MB concentration in the system varies from 0 to 0.1×10^{-3} M (Fig. 2). This trend indicates that the π-π stacking and possibly hydrophobic interactions are the main factors that contribute to the sequestration of MB, rather than electrostatic interactions. However, PDAC-SPS coacervates show a reduced sequestration capacity for BtB compared to that of MB, but there is also a trend of BtB partition coefficient increasing with BtB concentration in the system. Specifically, the BtB partition coefficient into PDAC-SPS coacervate increases from around 15 to 45, as the overall concentration of BtB varies from 0.01 to 0.1 mM. This comparatively low sequestration of BtB into PDAC-SPS coacervate suggests that the affinity of BtB for the coacervate is not as strong as that of MB.

The partition coefficient representing MB concentration in the PDAC-SPS coacervate compared to its concentration in the water rich phase was also studied as a function of PDAC:SPS molar ratio (Fig. S3). As the PDAC:SPS mixing ratio increases from 0.067 to 0.5, the partition coefficient of MB decreases from approximately 139 to 117. The decrease in the MB partition coefficient of MB with the increase in PDAC:SPS mixing ratio can be ascribed to the decreasing SPS content in the coacervate phase. The composition of the as-prepared PDAC-SPS coacervates was determined using ^{1}H NMR, as shown in Fig. S4. As the overall PDAC:SPS molar ratio in the system was increased from 0.067 to 0.5, the PDAC:SPS molar ratio in the coacervate phase increases from approximately 0.41 to 0.5 only, which does not vary as significantly as the overall molar ratio in the system. The zeta potential of the prepared PDAC-SPS coacervates with various overall PDAC:SPS ratio was measured as well (Fig. S5). The absolute zeta potential values of the PDAC-SPS coacervates decrease slightly as the overall PDAC:SPS molar ratio increases with a large range from 0.067 to 0.5, which corresponds to the slight variation of the coacervate composition obtained from ^{1}H NMR measurement.

3.2. Effect of solutes on zeta potential of PDAC-SPS coacervates

The apparent zeta potentials of the PDAC-SPS coacervates prepared with the addition of various concentrations of MB or BtB were measured, as shown in Fig. 2. An increase in MB concentration in the system results in a remarkable change in the zeta potential value of the PDAC-SPS coacervates, varying from approximately −36 to −5 mV as the concentration of MB increases from 0 to 0.1 mM. However, for the SPS-PDAC coacervates with the addition of BtB, the variation in zeta potential with the addition of BtB is much slighter than that of MB, changing from −36 to −25 mV only. These results are reasonable since the sequestered MB is positively charged while BtB is nonionic at the studied pH. Therefore, the dramatic decrease in the absolute zeta potential value of PDAC-SPS coacervates with the addition of MB is because of its positive charge. Additionally, even though the apparent zeta potential, which reflects the negative charge of the coacervate, is reduced from approximately −36 to −5 mV as the overall concentration in the system increases from 0 to 0.1 mM, the partition coefficient of MB into PDAC-SPS coacervates still keeps increasing. This trend indicates that the π-π stacking and possibly hydrophobic interactions are the main factors that contribute to the sequestration of MB, rather than electrostatic interactions, since the coacervate with low negative charge still uptake MB with a high efficiency. The UV–vis spectra of BtB in aqueous solution at different pH values as well as that for BtB in PDAC aqueous solution at pH = 3.0 are shown in Fig. S2. BtB acts as a weak acid in aqueous solution ($pK_a = \sim 7.1$) [17], which can thus be in protonated or deprotonated form, appearing yellow or blue respectively. The UV–vis peak at 433 nm is attributed to the protonated form of BtB, while the peak at 617 nm is assigned to the deprotonated form of BtB. However, since at the experimental pH value (pH = 3) BtB is nonionic in both pure aqueous solution and PDAC solution, it is unclear what the cause of the change in absolute zeta potential value of PDAC-SPS coacervate is as the concentration of BtB in the system increases. To better explain this phenomenon, ITC experiments were carried out to better understand the interaction between the dyes and polyelectrolytes used in this study.

3.3. Isothermal titration calorimetry (ITC)

ITC was employed to study the intermolecular interaction of MB and BtB with PDAC and SPS. ITC is able to show whether an association process occurs between two molecules and allows for estimation of the intermolecular interaction strength between the dyes and polyelectrolytes. Fig. 3 shows the ITC titration curves for the titration of the polyelectrolyte (PDAC or SPS) solutions into dye (MB or BtB) solutions. The ordinate axis represents the enthalpy changes due to the polyelectrolyte injection, and the abscissa is the corresponding composition of the system (polyelectrolyte monomer:dye ratio). Based on these results, there is no enthalpy change for the titration of PDAC into MB and SPS into BtB solution, indicating that there is no specific intermolecular interaction between MB and PDAC or BtB and SPS, or the interaction is too weak to be detected by ITC. However, both the titration of SPS into MB and PDAC into BtB shows a significant exothermic signal, which is an indication of a substantial polyelectrolyte-dye interaction. In both dye-polymer systems, saturation (where the exothermic binding heat diminishes to baseline levels) occurs near the 1:1 polyelectrolyte:dye ratio, suggesting that the binding sites for the MB and BtB dye molecules do not exceed one polyelectrolyte monomer unit in size. The titration of PDAC into BtB has a less negative profile than that of SPS into MB, suggesting that the interaction between MB and SPS is much stronger than that for BtB and PDAC. However, as entropy plays a large role in the interactions here, it is important to also note that this greater interaction strength is also supported by a more abrupt saturation transition [18], which is indicative of stronger binding and is consistent with the much higher partition coefficient of MB into PDAC-SPS coacervate than that of BtB.

It is a little surprising to see such a strong association between PDAC and BtB since at pH 3.0, BtB is non-ionized, as indicated in Fig. S2. It was reported that PDAC is capable of forming cation-π interactions with aromatic molecules such as reduced graphene oxide, charged and uncharged lignin [19,20]. Additionally, a careful

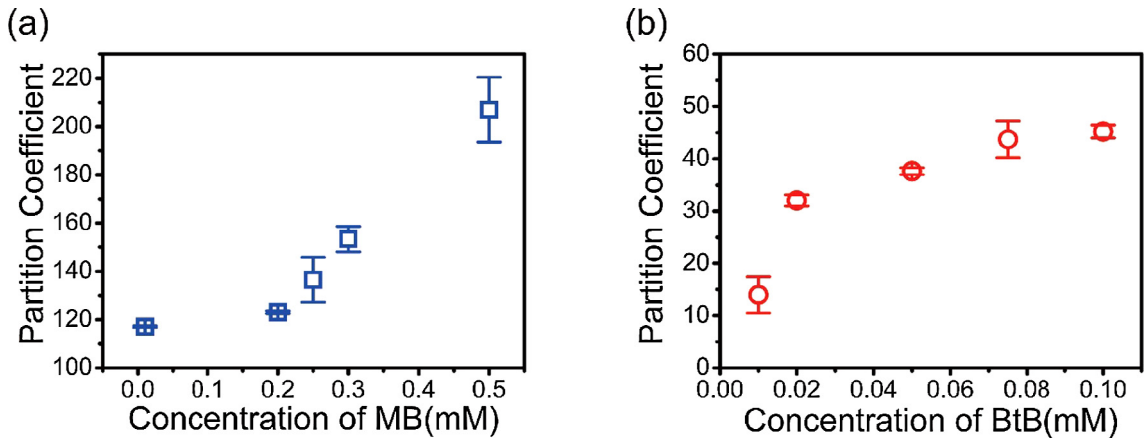

Fig. 1. Partition coefficient of (a) MB and (b) BtB into PDAC-SPS coacervates as a function of various concentration of MB or BtB. PDAC-SPS coacervates were prepared using PDAC (10 mM) and SPS (10 mM) stock solution with a mixing ratio of PDAC : SPS = 00.5.

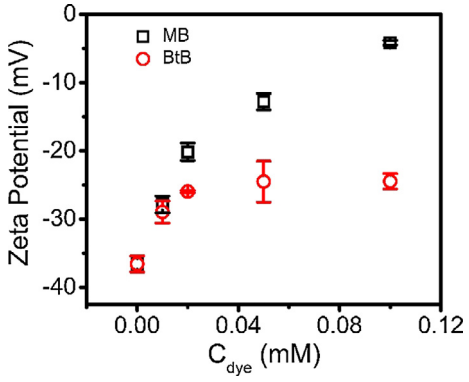

Fig. 2. Zeta potential of PDAC-SPS coacervates with the addition various concentration of MB or BtB. PDAC-SPS coacervates were prepared using PDAC (10 mM) and SPS (10 mM) stock solution with a mixing ratio of PDAC : SPS = 00.5.

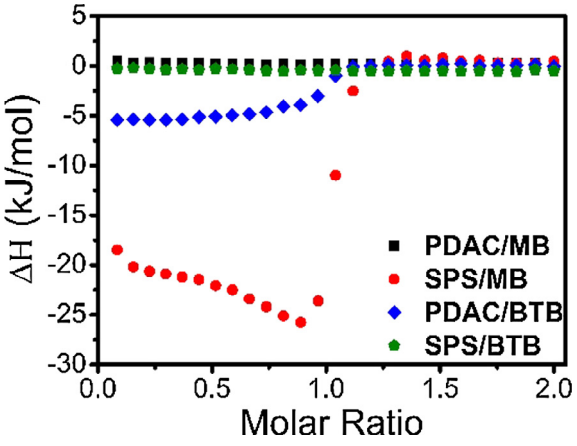

Fig. 3. ITC data for the titration of 2.5 mM PDAC or SPS into 0.25 mM MB or BtB solution.

observation of the titration curve of SPS into MB (where the enthalpic signal increases in magnitude up to the stoichiometric point) reveals that binding of MB to SPS occurs in two steps. It has been reported that in aqueous solution, MB undergoes exothermic dimerization and trimerization at MB concentration higher than 0.1 mM [21,22], with similar orders of magnitude as the dye concentration in the ITC experiment. Addition of SPS into MB aqueous solution may therefore result in destruction of the MB dimer and trimer, with the formation of SPS-MB associations via π-π stacking and electrostatic interaction [23]. The breakup of dimer and trimer at low SPS:MB ratio could absorb heat and therefore reduce the net exothermic signal [22]. At higher SPS:MB ratios, the concentration of MB that is unbound to SPS becomes lower, which corresponds to fewer MB aggregates in solution. Thus, fewer MB aggregates likely break up at high SPS:MB ratios, and with less heat absorbed by this unstacking process, the net exothermic signal increases.

3.4. Effect of accumulated MB on the hydrophobicity within PDAC-SPS coacervate droplets

Generally, the partition coefficient of solutes into coacervates decreases as the solution concentration in the system increases. For example, it was reported that the encapsulation efficiency of BSA protein into polypeptide coacervates decreases as the ratio of BSA to polypeptide increases [24]. However, in our PDAC-SPS coacervate system with MB, the partition coefficient of MB was significantly increased as the concentration of MB in the system increases, which is unusual at first sight. An assumption that arises is that the accumulated MB within PDAC-SPS coacervates is capable of influencing the chemical environment of the coacervate and therefore further uptake the MB molecules in aqueous solution into PDAC-SPS coacervate droplets, resulting in such a high sequestration efficiency even at high MB concentrations.

To study how the accumulated MB can influence the environment within the coacervate, fluorescence spectra of ANS sequestered within the PDAC-SPS coacervate droplets with the presence of different concentration of MB in the system were measured, as shown in Fig. 4. The photo-physical properties of are highly sensitive to polarity and viscosity of the environment. As shown in Fig. 4, the fluorescence spectra of ANS sequestered within PDAC-SPS coacervates with the addition of different concentration of MB showed a broad emission band between 365 and 650 nm, which indicates a combination of different micro-environments of varying polarities within coacervate droplets. Deconvolution of the fluorescence spectra by Gaussian fitting provides two specific emission peaks associated with two distinct microenvironments of the coacervates. The peak located at ~470 nm was assigned to the nonpolar excited state localized on the naphthalene ring of ANS, which represents a more hydrophobic environment, which the other peak at ~530 nm was consistent with the emission from the charge transfer state of ANS, which corresponds to a more hydrophilic environment. As previously mentioned, the partition coefficient of MB into PDAC-SPS coacervates increases with the feed concentration of MB. It is therefore no doubt that

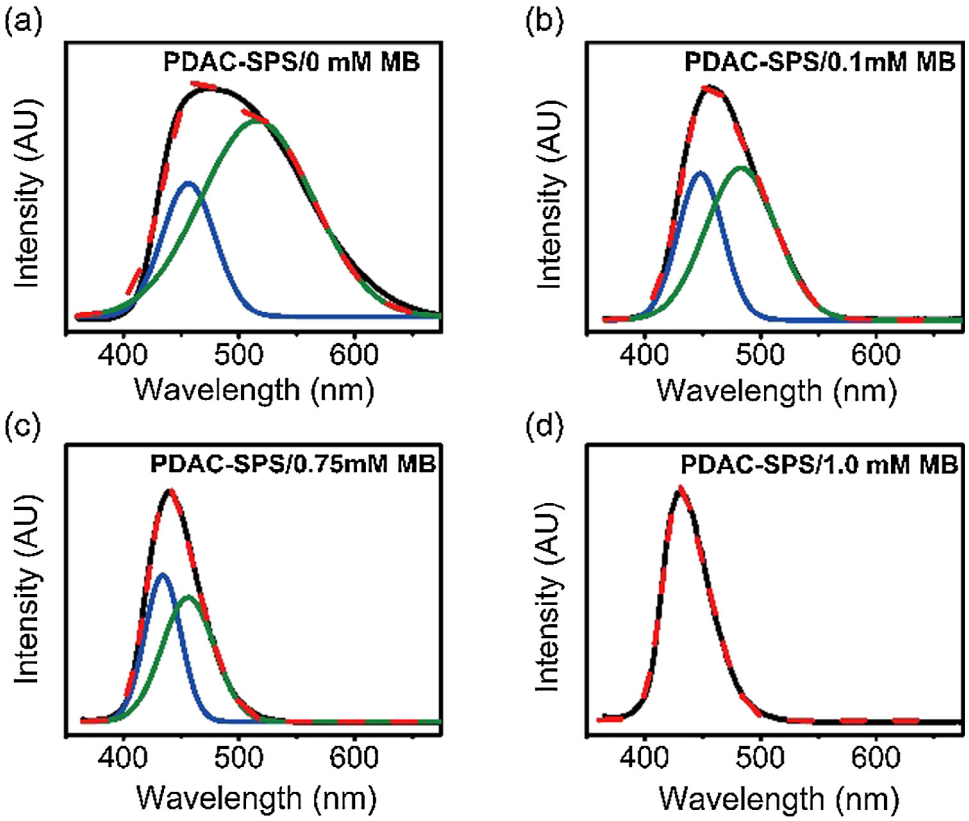

Fig. 4. Fluorescence emission spectra of ANS sequestered in PDAC-SPS coacervate dispersions with the addition of (a) 0 mM, (b) 0.1 mM, (c) 0.75 mM and (d) 1.0 mM MB recorded at room temperature. The coacervates were prepared with 10 mM PDAC and 10 mM SPS at a mixing ratio of PDAC:SPS = 0.5, with the addition of 0.5 mM ANS.

the sequestered amount of MB within the coacervates also increases with the overall MB concentration. As shown in Fig. 4, as the MB concentration increases from 0 to 1.0 mM, the relative intensity of emission peak at around 470 nm increases gradually, while the intensity of emission peak at approximately 530 nm attributed to the hydrophilicity or polarity of the environment within coacervate decreases to almost zero, indicating that the accumulated MB within coacervate droplets would increase the hydrophobicity of coacervate significantly. The enhanced hydrophobicity within PDAC-SPS coacervates induced by the accumulated MB would in turn enable the coacervates to uptake more MB, leading to a significantly increased MB partition coefficient with the increase of MB concentration.

3.5. Effect of solutes on PDAC-SPS phase behavior

The phase behavior of PDAC-SPS in the presence of added dye, with respect to the overall dye concentration, PDAC/SPS mixing ratio, and the total polyelectrolyte concentration, is illustrated and compared in a series of phase diagrams depicted in Figs. 5 and S6. Fig. S7 shows typical optical micrographs of precipitates and coacervates coexisting, or possibly aggregates of coacervate drops, prepared using PDAC and SPS aqueous solution. There are several characteristic features of the phase behavior of the PDAC-SPS system with the addition of MB or BtB.

First of all, for all PDAC-SPS concentrations studied here, the single-phase solution regime narrows with increasing MB or BtB concentration, indicating that the presence of MB or BtB slightly favors the coacervation process. Additionally, the broadening in the precipitation regime with increasing MB or BtB concentration suggests that the presence of MB or BtB strongly favors precipitation. The increase in ionic strength induced by the positively charged MB should not be the main factor that impacts the phase behavior of the PDAC-SPS system, since the addition of 1 mM NaCl into the polyelectrolyte system has almost no impact on the phase diagram, as shown in Fig. S6. Increased hydrophobicity of coacervates with the addition of dyes is suggested as the main reason for the acceleration of coacervation. It has been reported that an increase in the hydrophobicity of polyelectrolytes increases the tendency towards coacervation despite the reduction in charge interactions between the polyelectrolytes [25]. Additionally, the tendency towards precipitation was also enhanced as the concentration of MB or BtB in the system increases. There are multiple reasons for the increase in the tendency towards precipitation. Firstly, an increase in the MB or BtB concentration of the system leads to a lower absolute value of zeta potential of the coacervates, resulting in weaker electrostatic repulsion between coacervates, which might accelerate the precipitation. Secondly, the increased hydrophobicity of the coacervates by the addition of dyes might also contributes to the enhancement of tendency towards precipitation.

Second, the total polyelectrolyte concentration has an impact on the phase behavior of PDAC-SPS system as well. An increase in coacervate formation as reflected by turbidity with increasing total polymer concentration was observed for all MB and BtB concentrations. One example of the influence of polyelectrolyte total concentration on the turbidity of PDAC-SPS system is shown in Fig. S8. Additionally, a higher total polyelectrolyte concentration promotes coacervation and precipitation, as shown in Fig. S6. Mixtures with higher polymer concentrations have a higher number of oppositely charged sites available to interact, thus the coacervation and precipitation tend to occur earlier at a smaller PDAC to SPS ratio.

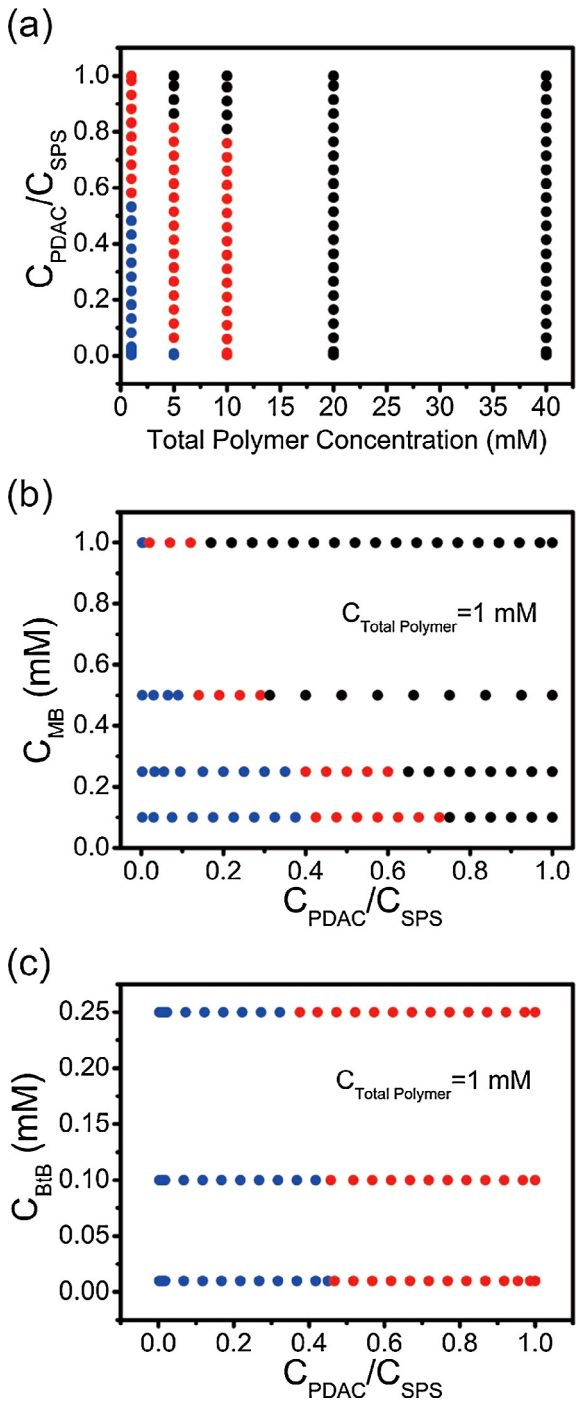

Fig. 5. (a) Phase behavior of PDAC-SPS aqueous system as a function of polyelectrolyte stoichiometry, total polymer concentration, and phase behavior of PDAC-SPS aqueous system as a function of overall concentration of dye (b) MB or (c) BtB and polyelectrolyte stoichiometry. Blue (●), red (●) and black (●) symbols represent clear solution, coacervation and precipitation, respectively. (For interpretation of the references to color in this figure legend, the reader is referred to the web version of this article.)

3.6. Effect of MB and BtB on water content of coacervates

Experimentally, the water content of ternary coacervate is determined simply by weighing the complex coacervate before and after drying. Fig. S9 shows the water content of PDAC-SPS coacervates as a function of concentration of MB or BtB in the system. In general, an increase in the concentration of MB or BtB results in a decrease in water content of the formed PDAC-SPS coacervates. To be specific, the water content of PDAC-SPS complex coacervate is reduced from approximately 86.9% to 64.6% as the concentration of MB increases from 0 to 0.5 mM. Similarly, the water content of PDAC-SPS coacervates is reduced from 86.9% to 76.0% with an increase in the concentration of BtB from 0 to 0.2 mM. This can be considered an indirect proof that the hydrophobicity of PDAC-SPS coacervates with the sequestered BtB might also be increased as the concentration of BtB increases.

3.7. Effect of solutes on the rheological properties of complex coacervates

It has been reported that the rheological properties of polyelectrolyte complexes and coacervates are influenced by various factors, including salt concentration, polyelectrolyte stoichiometry and pH [26–28]. Dynamic rheological measurements were used to characterize the coacervate materials, as shown in Figs. 6 and 7. The frequency sweep was performed at a constant strain of 0.4%, which was found to be in the linear regime. The viscoelastic behavior is highly dependent on the addition of MB or BtB.

The presence of MB within the complex coacervates has a strong influence on the rheological properties of PDAC-SPS coacervates. The frequency sweep data shows a decrease in the overall magnitude of the storage (G′) and loss (G″) moduli with increasing MB concentration (Fig. 6a), which is similar to the salt effect on the rheological properties of coacervates, although enhanced given the low overall concentration of dye [29–31]. Furthermore, for the PDAC-SPS coacervate samples prepared at high MB concentrations (0.4 and 0.5 mM), a frequency-dependent crossover between the storage and loss moduli can be observed, while at lower MB concentrations, the storage modulus was dominant over the entire frequency range, indicating the coacervate samples prepared at low MB concentrations are more solid-like. For the coacervate samples prepared at high MB concentrations, at low frequencies the loss modulus dominates over the storage modulus, indicative of a viscoelastic liquid-like behavior, while at higher frequencies, a crossover in the two moduli was observed, followed by a region where solid-like behavior dominates. Additionally, as shown in Fig. 7a, $\tan(\delta)$ of PDAC-SPS coacervates formed at various concentration of MB all exhibit a decrease with increasing frequency. At low MB concentrations (0, 0.1 and 0.2 mM) $\tan(\delta)$ is much lower than 1, indicative of solid-like feature of the coacervate. However, for PDAC-SPS coacervates prepared at high MB concentrations (0.4 and 0.5 mM), $\tan(\delta)$ is higher than 1, indicating a viscoelastic liquid-like behavior, while at high frequencies the $\tan(\delta)$ is lower than 1, with solid-like behavior dominating. Plotting $\tan(\delta)$ data as a function of MB concentration instead of the frequency can help with visualization and elucidation of the relation between the crossover frequency and MB concentration (Fig. 8). The crossover frequency increases as the concentration of MB increases. The inverse of the crossover frequency (where $\tan(\delta) = 1$) can be related to the longest relaxation time for the polymers in the sample [30]. Here, an observation of increasing crossover frequency for increasing MB concentration corresponds to a decrease in the time needed for polymer molecules to disentangle and relax. As mentioned before, an increase in the MB concentration results in a decrease in water content of the formed PDAC-SPS coacervates. If water is to be considered as a plasticizer for polyelectrolyte complexes [32–34], a lower water content should lead to a higher coacervate modulus. However, in this study, as the concentration of MB increases, though the water content is reduced, the overall magnitude of the storage (G′) and loss (G″) moduli decrease with increasing MB concentration. This unusual behavior indicates that the MB encapsulated within PDAC-SPS coacervates tends to efficiently impair the ionic bond between PDAC and SPS. The wt% of MB

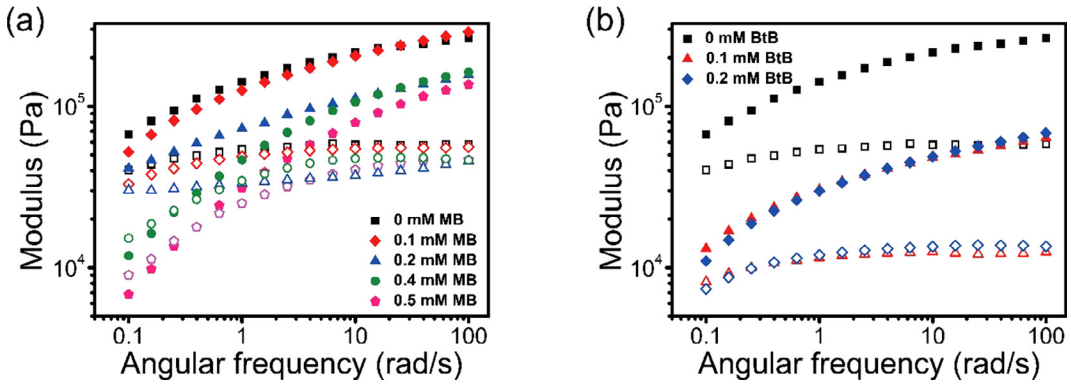

Fig. 6. Frequency sweeps showing storage (G′, solid) and loss (G″, open) modulus of PDAC-SPS coacervates formed by mixing 5 mM PDAC stock solution and 5 mM SPS stock solution at a stoichiometry of PDAC : SPS = 0.75 with the addition of (a) various concentration of MB, and (b) various concentration of BtB.

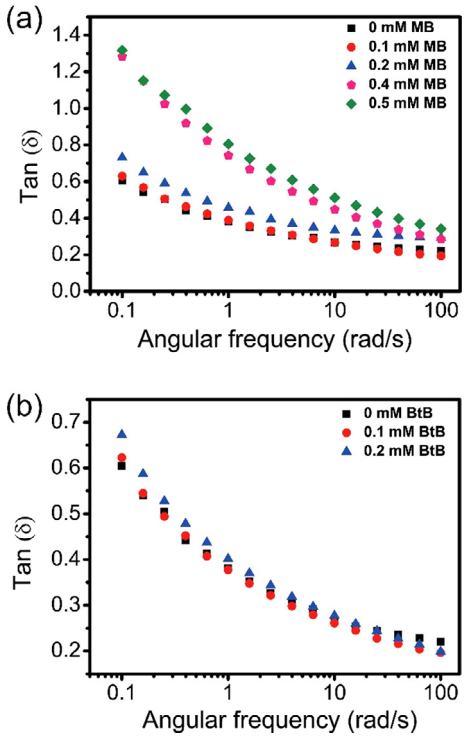

Fig. 7. Loss tangent ($\tan(\delta) = G''/G'$) of the PDAC-SPS coacervates formed with various concentration of MB or BtB.

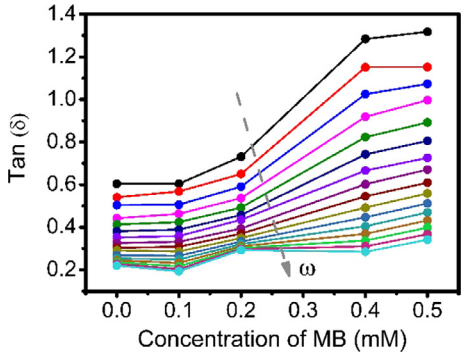

Fig. 8. Plot of loss tangent ($\tan(\delta) = G''/G'$) of the PDAC-SPS coacervates as a function of MB concentrations. Data are shown for angular frequencies ranging from 0.1 to 100 rad/s.

molecules in the PDAC-SPS coacervates is quite low, varying from 0.03% to 2.38% as the overall MB concentration in the system increases from 0.01 to 0.5 mM, which indicates that the displacement of ionic bond pairs between the oppositely charged polyelectrolytes by the positively charged MB is limited. In addition to the displacement of ionic bond pairs by MB, the formation of ionic bond pairs between PDAC and SPS is further sterically hindered by the MB molecules which associates with SPS through both ionic and π-π interaction.

Similarly, with the increase in concentration of BtB in the coacervate, though the water content of the PDAC-SPS coacervate decreases, there is still a decrease in the overall magnitude of the storage (G′) and loss (G″) moduli and a slight increase in the tan(δ) (Figs. 6b and 7b), indicating that the presence of BtB within PDAC-SPS coacervates reduces the ionic crosslink density of the PDAC-SPS material, because of the cation-π interaction between PDAC and BtB. The cation-π interaction is electrostatic in nature, which can be conceptualized as the interaction of a positively charged ion with the negative electrostatic potential surface of the π electrons above and below the aromatic structure [35,36]. Therefore, as with the MB case, the cation-π interaction between PDAC and BtB leads to a weaker interconnecting network of the PDAC-SPS coacervates as the concentration of BtB increases.

4. Conclusion

It has been widely reported that coacervates are capable of encapsulation of various solutes, including small organic molecules, proteins, and nanoparticles [12,13,24,37,38]. Previous studies reveal that phase behavior of complex coacervation is dependent on various factors, such as ionic strength, polymer molecular weight, pH, temperature, as well as the polymer concentration [1,14]. However, there are few studies on how the sequestered solutes within coacervates would in turn impact the phase behavior and coacervation of aqueous polyelectrolyte systems. Presented here is a study of the sequestration of the small molecules MB and BtB into PDAC-SPS complex coacervate, as well as the influence of the sequestered solutes on the phase behavior and properties of the coacervate. The absolute apparent zeta potential values of the PDAC-SPS coacervates decrease as the concentration of MB or BtB in the system increases. Hydrophobicity within the PDAC-SPS coacervate droplets can be increased simply by increasing the sequestered MB content within the complex coacervate. The phase behavior of PDAC-SPS system is highly dependent on the concentration of dyes as well as the total polyelectrolyte concentration. An increase in the MB or BtB concentration of the system tends to shift the window over which

coacervation and precipitation occur to a wider range of stoichiometric ratios of oppositely charged polyelectrolyte. Additionally, for mixtures with higher total polyelectrolyte concentration, coacervation and precipitation tend to occur earlier at a smaller PDAC to SPS ratio. The accumulation of MB or BtB within PDAC-SPS coacervate phase has a strong influence on the rheological properties of the coacervates. As the concentration of MB or BtB increases, there is a decrease in the overall magnitude of the storage (G') and loss (G'') moduli and an increase in the $\tan(\delta)$, indicating that the presence of these two small molecules within PDAC-SPS coacervates can reduce the ionic bonds between PDAC and SPS. In conclusion, this work studies the encapsulation of solutes into coacervates as well as the influence of the sequestered solutes on the phase behavior of the polyelectrolyte solution, hydrophobicity within coacervate droplets, as well as the rheological properties of the coacervates, which may provide some guidance for design of solute-encapsulated coacervates with desired properties.

Acknowledgements

The authors would like to acknowledge support from NSF award DMR-1425187 as well as thank Prof. Xiong Gong of the University of Akron for use of his UV–vis equipment, Prof. Bryan Vogt and Chao Wang for help with rheology, and Prof. David Dignam of the University of Toledo for the use of his ITC.

Appendix A. Supplementary material

Supplementary data associated with this article can be found, in the online version, at https://doi.org/10.1016/j.jcis.2018.02.029.

References

[1] R. Chollakup, J.B. Beck, K. Dirnberger, M. Tirrell, C.D. Eisenbach, Polyelectrolyte molecular weight and salt effects on the phase behavior and coacervation of aqueous solutions of poly(acrylic acid) sodium salt and poly(allylamine) hydrochloride, Macromolecules 46 (2013) 2376–2390, https://doi.org/10.1021/ma202172q.
[2] Y. Wang, K. Kimura, P.L. Dubin, W. Jaeger, Polyelectrolyte-micelle coacervation: effects of micelle surface charge density, polymer molecular weight, and polymer/surfactant ratio, Macromolecules 33 (2000) 3324–3331, https://doi.org/10.1021/ma991886y.
[3] E. Kizilay, A.B. Kayitmazer, P.L. Dubin, Complexation and coacervation of polyelectrolytes with oppositely charged colloids, Adv. Colloid Interface Sci. 167 (2011) 24–37, https://doi.org/10.1016/j.cis.2011.06.006.
[4] D. Priftis, N. Laugel, M. Tirrell, Thermodynamic characterization of polypeptide complex coacervation, Langmuir 28 (2012) 15947–15957, https://doi.org/10.1021/la302729r.
[5] L. Vitorazi, N. Ould-Moussa, S. Sekar, J. Fresnais, W. Loh, J.-P. Chapel, J.-F. Berret, Evidence of a two-step process and pathway dependency in the thermodynamics of poly(diallyldimethylammonium chloride)/poly(sodium acrylate) complexation, Soft Matter 10 (2014) 9496–9505, https://doi.org/10.1039/c4sm01461h.
[6] J. van der Gucht, E. Spruijt, M. Lemmers, M.A. Cohen, Stuart, Polyelectrolyte complexes: bulk phases and colloidal systems, J. Colloid Interface Sci. 361 (2011) 407–422, https://doi.org/10.1016/j.jcis.2011.05.080.
[7] J. Požar, D. Kovačević, Complexation between polyallylammonium cations and polystyrenesulfonate anions: the effect of ionic strength and the electrolyte type, Soft Matter 10 (2014) 6530–6545, https://doi.org/10.1039/c4sm00651h.
[8] F. Shahidi, J.K.V. Arachchi, Y.J. Jeon, Food applications of chitin and chitosans, Trends Food Sci. Technol. 10 (1999) 37–51, https://doi.org/10.1016/S0924-2244(99)00017-5.
[9] S.A. Agnihotri, N.N. Mallikarjuna, T.M. Aminabhavi, Recent advances on chitosan-based micro- and nanoparticles in drug delivery, J. Control. Release 100 (2004) 5–28, https://doi.org/10.1016/j.jconrel.2004.08.010.
[10] B.P. Koppolu, S.G. Smith, S. Ravindranathan, S. Jayanthi, T.K. Suresh Kumar, D. A. Zaharoff, Controlling chitosan-based encapsulation for protein and vaccine delivery, Biomaterials 35 (2014) 4382–4389, https://doi.org/10.1016/j.biomaterials.2014.01.078.
[11] Y. Yeo, E. Bellas, W. Firestone, R. Langer, D.S. Kohane, Complex coacervates for thermally sensitive controlled release of flavor compounds, J. Agric. Food Chem. 53 (2005) 7518–7525, https://doi.org/10.1021/jf0507947.
[12] M. Zhao, N.S. Zacharia, Sequestration of methylene blue into polyelectrolyte complex coacervates, Macromol. Rapid Commun. 37 (2016) 1249–1255, https://doi.org/10.1002/marc.201600244.
[13] M. Zhao, S.A. Eghtesadi, M.B. Dawadi, C. Wang, S. Huang, A.E. Seymore, B.D. Vogt, D.A. Modarelli, T. Liu, N.S. Zacharia, Partitioning of small molecules in hydrogen-bonding complex coacervates of poly(acrylic acid) and poly(ethylene glycol) or pluronic block copolymer, Macromolecules 50 (2017) 3818–3830, https://doi.org/10.1021/acs.macromol.6b02815.
[14] R. Chollakup, W. Smitthipong, C.D. Eisenbach, M. Tirrell, Phase behavior and coacervation of aqueous poly(acrylic acid)-poly(allylamine) solutions, Macromolecules 43 (2010) 2518–2528, https://doi.org/10.1021/ma902144k.
[15] D. Priftis, K. Megley, N. Laugel, M. Tirrell, Complex coacervation of poly(ethylene-imine)/polypeptide aqueous solutions: thermodynamic and rheological characterization, J. Colloid Interface Sci. 398 (2013) 39–50, https://doi.org/10.1016/j.jcis.2013.01.055.
[16] Q. Wang, J.B. Schlenoff, The polyelectrolyte complex/coacervate continuum, Macromolecules 47 (2014) 3108–3116, https://doi.org/10.1021/ma500500q.
[17] G.S. Patterson, A simplified method for finding the pKa of an acid-base indicator by spectrophotometry, J. Chem. Educ. 76 (1999) 395, https://doi.org/10.1021/ed076p395.
[18] T. Wiseman, S. Williston, J.F. Brandts, L.N. Lin, Rapid measurement of binding constants and heats of binding using a new titration calorimeter, Anal. Biochem. 179 (1989) 131–137, https://doi.org/10.1016/0003-2697(89)90213-3.
[19] J.P.C. Trigueiro, R.L. Lavall, G.G. Silva, Supercapacitors based on modified graphene electrodes with poly(ionic liquid), J. Power Sources 256 (2014) 264–273, https://doi.org/10.1016/j.jpowsour.2014.01.083.
[20] K.V. Pillai, S. Renneckar, Cation-π interactions as a mechanism in technical lignin adsorption to cationic surfaces, Biomacromolecules 10 (2009) 798–804, https://doi.org/10.1021/bm801284y.
[21] E. Braswell, Evidence for trimerization in aqueous solutions of methylene blue, J. Phys. Chem. 72 (1968) 2477–2483, https://doi.org/10.1021/j100853a035.
[22] P. Mukerjee, A.K. Ghosh, P. Mukerjee, A.K. Ghosh, Thermodynamic aspects of the self-association and hydrophobic bonding of methylene blue. A model system for stacking interactions, J. Am. Chem. Soc. 92 (1970) 6419–6424, https://doi.org/10.1021/ja00725a006.
[23] M. Shirai, T. Nagatsuka, M. Tanaka, Interaction between dyes and polyelectrolytes, 2) structural effect of polyanions on the methylene blue binding, Makromol. Chem. 178 (1976) 37–46.
[24] K.A. Black, D. Priftis, S.L. Perry, J. Yip, W.Y. Byun, M. Tirrell, Protein encapsulation via polypeptide complex coacervation, ACS Macro Lett. 3 (2014) 1088–1091, https://doi.org/10.1021/mz500529v.
[25] P.K. Jha, P.S. Desai, J. Li, R.G. Larson, pH and salt effects on the associative phase separation of oppositely charged polyelectrolytes, Polymers (Basel) 6 (2014) 1414–1436, https://doi.org/10.3390/polym6051414.
[26] H. Zhang, C. Wang, G. Zhu, N.S. Zacharia, Self-healing of bulk polyelectrolyte complex material as a function of pH and salt, ACS Appl. Mater. Interfaces 8 (2016) 26258–26265, https://doi.org/10.1021/acsami.6b06776.
[27] C. Wang, Y. Duan, N.S. Zacharia, B.D. Vogt, A family of mechanically adaptive supramolecular graphene oxide/poly(ethylenimine) hydrogels from aqueous assembly, Soft Matter 13 (2017) 1161–1170, https://doi.org/10.1039/C6SM02439D.
[28] M.W. Liberatore, N.B. Wyatt, M. Henry, P.L. Dubin, E. Foun, Shear-induced phase separation in polyelectrolyte/mixed micelle coacervates, Langmuir 25 (2009) 13376–13383, https://doi.org/10.1021/la903260r.
[29] E. Spruijt, M.A. Cohen Stuart, J. Van Der Gucht, Linear viscoelasticity of polyelectrolyte complex coacervates, Macromolecules 46 (2013) 1633–1641, https://doi.org/10.1021/ma301730n.
[30] Y. Liu, H.H. Winter, S.L. Perry, Linear viscoelasticity of complex coacervates, Adv. Colloid Interface Sci. 239 (2017) 46–60, https://doi.org/10.1016/j.cis.2016.08.010.
[31] Y. Liu, B. Momani, H.H. Winter, S.L. Perry, Rheological characterization of liquid-to-solid transitions in bulk polyelectrolyte complexes, Soft Matter 13 (2017) 7332–7340, https://doi.org/10.1039/C7SM01285C.
[32] H.H. Hariri, A.M. Lehaf, J.B. Schlenoff, Mechanical properties of osmotically stressed polyelectrolyte complexes and multilayers: water as a plasticizer, Macromolecules 45 (2012) 9364–9372, https://doi.org/10.1021/ma302055m.
[33] P. Schaaf, J.B. Schlenoff, Saloplastics: processing compact polyelectrolyte complexes, Adv. Mater. 27 (2015) 2420–2432, https://doi.org/10.1002/adma.201500176.
[34] Y. Zhang, F. Li, L.D. Valenzuela, M. Sammalkorpi, J.L. Lutkenhaus, Effect of water on the thermal transition observed in poly(allylamine hydrochloride)-poly(acrylic acid) complexes, Macromolecules 49 (2016) 7563–7570, https://doi.org/10.1021/acs.macromol.6b00742.
[35] P.B. Crowley, A. Golovin, Cation – π interactions in protein – protein, Interfaces 239 (2005) 231–239, https://doi.org/10.1002/prot.20417.
[36] M. Keiluweit, M. Kleber, Molecular-level interactions in soils and sediments: the role of aromatic π-systems, Environ Sci Technol 43 (2009) 3421–3429.
[37] K. Lv, A.W. Perriman, S. Mann, Photocatalytic multiphase micro-droplet reactors based on complex coacervation, Chem. Commun. 51 (2015) 8600–8602, https://doi.org/10.1039/C5CC01914A.
[38] N. Martin, M. Li, S. Mann, Selective uptake and refolding of globular proteins in coacervate microdroplets, Langmuir 32 (2016) 5881–5889, https://doi.org/10.1021/acs.langmuir.6b01271.